

Evaluation of atmospheric blocking over the Northeast Pacific in the CFS and AMIP model simulations

M. L. Carrera, N. Gaggini, and R. W. Higgins

Climate Prediction Center
NOAA/NWS/NCEP, Camp Springs, MD, USA

1.0 Introduction

Episodes of prolonged extreme weather conditions, such as droughts, floods and heat waves are of considerable importance to society. It is now widely recognized that such weather extremes are often associated with recurrent atmospheric flow anomalies (Dole 1986; Higgins and Schubert 1994, 1996; Robertson and Ghil 1999) that can last from several days up to a few weeks.

One feature that is often implicated in these events is the persistent anticyclonic flow anomaly, which is often referred to as an atmospheric “blocking” episode (Dole 1986; Higgins and Schubert 1996; Higgins and Mo 1997). Atmospheric blocking refers to the situation where the normal zonal flow is interrupted by strong and persistent meridional flow. The normal eastward progression of synoptic disturbances is obstructed, as the systems are forced to the north and south of the blocking anticyclone, leading to anomalous storm tracks (Nakamura and Wallace 1990).

Numerous studies have alluded to the inherent problems of numerical weather prediction models in forecasting events of atmospheric blocking (Tibaldi and Molteni 1990; Tibaldi et al. 1994; Chen and Van den Dool 1995; D’Andrea et al. 1998). A finding common to most studies is that medium-range forecast models underestimate the observed blocking frequency owing to their inherent problems in transitioning to a blocked state. Recently, with the introduction of ensemble forecasting systems at both the National Centers for Environmental Prediction (NCEP) and at the European Centre for Medium-Range Weather Forecasts (ECMWF), the forecasting of atmospheric blocking at the medium ranges has improved (Watson and Colucci 2002; Pelly and Hoskins 2003).

In this study we build upon the recent study of Carrera et al. (2004) which examined the downstream weather impacts associated with atmospheric blocking over the Alaskan region of the Northeast Pacific during the boreal winter. In that study the authors showed that Alaskan blocking was associated with an equatorward shift of the Pacific storm track, and significant downstream development of 500-hPa geopotential height, and sea-level pressure anomalies over North America. Here we assess how well two recent long-term model integrations, perform in reproducing the Alaskan blocking-circulation relationships found in observations.

2.0 Data and Methodology

The NCEP-National Center for Atmospheric Research (NCAR) reanalysis (Kalnay et al. 1996; hereafter referred to as the NCEP reanalysis) daily averaged 500-hPa geopotential heights for the 22-yr period 1979-2000 are used to identify observed events of atmospheric blocking. Following the recent article by Kistler et al. (2001), which concluded that the reanalysis climatology after 1979 was the most reliable, owing to the introduction of satellite data, we restrict the analysis to the period from 1979 onward.

A global gridded daily maximum and minimum surface temperature dataset over land at 2.5° latitude-longitude resolution is used to document the temperature impacts associated with the Alaskan blocking regime. The data begin in 1979 and are derived from “first order” World Meteorological Organization (WMO) meteorological recording stations received over the Global Telecommunication System (GTS), with typically between 6000-7000 stations reporting daily, including roughly 950 stations over the North American region

(15°-90°N, 60°-170°W). This dataset will be referred to as the GTS dataset.

Precipitation impacts are assessed via the newly completed North American Regional Reanalysis (RR) (Mesinger et al. 2004). The RR is a long-term homogeneous mesoscale regional analysis performed with a frozen state-of-the-art model and data assimilation system. The domain covers North America and the adjacent oceans. The model used is the NCEP operational Eta model of 2003, which has a horizontal resolution of 32 km and 45 layers in the vertical. One of the unique features of the RR system is the direct assimilation of observed precipitation. The RR website provides more details on the RR system (<http://wwwt.emc.ncep.noaa.gov/mmb/rrean/>).

The two long-term model integrations used in this study are the free-run of the newly implemented NCEP Coupled Forecast Model (CFS) and an AMIP type run with the GFS (Global Forecast System) model. The components of the CFS model are the T62/64 layer version of the current NCEP atmospheric GFS combined with the 40-level GFDL (Geophysical Fluid Dynamics Laboratory) Modular Ocean Model (MOM) version 3. Direct coupling is done once per day with no flux correction. The CFS free-run was initialized with data on 1 January 2002 and run out for 32 years. To compare with the 22-year observed period (1979-2000) from NCEP, we use the data from 2004-2025.

The AMIP simulation was performed with the T62/64 layer GFS model (~operational version of March 2003) for the period 1949-2000. Weekly observed SSTs were from the analysis of Smith and Reynolds. To be consistent with the Alaskan blocking events in the NCEP reanalysis, we examine the AMIP-II simulations for the period 1979 to 2000.

To identify blocking events over the Alaskan region of the Northeast Pacific in both the observations and model integrations, we use the threshold crossing procedure of Dole and Gordon (1983) applied to the 500-hPa geopotential height anomaly field. For this study, the threshold and duration criteria chosen were 100 m and 8 days. Prior to applying the threshold

crossing procedure, the 500-hPa height anomaly fields were calculated by first removing the local seasonal cycle, defined as the mean plus the annual and semiannual harmonics of the respective 22 year mean annual cycles, and then applying a 10-day low-pass Lanczos filter with 121 weights. The key point chosen in the Northeast Pacific is located at 62.5°N and 162.5°W, centered over extreme western Alaska. A plot of the geographical distribution of the total number of persistent positive 500-hPa geopotential height anomaly events (i.e., blocking events) satisfying the selection criteria of (100 m, 8 days) for the December-March (DJFM) period from 1979 to 2000 in the observations (not shown) revealed this location as a local maximum.

We restricted our analysis to those blocking events with onset times, that is, the time when the 500-hPa geopotential height anomaly first crosses the threshold of 100 m, in DJFM. Table 1 summarizes the results from the observations and model integrations.

Model	Time Period	# of Blocking Events	Mean Duration (days)
NCEP	1979-2000	37	11.3
AMIP	1979-2000	37	11.3
CFS	2004-2025	27	13.7

Table 1. Summary of atmospheric blocking events for the key point located at 62.5°N, 162.5°W in the Northeast Pacific.

Examining table 1, we note the CFS model simulates a reduced number of Alaskan blocking events (37 vs 27) with a larger mean duration, when compared to the observed and the AMIP simulation.

3. Composite structure

a. 500-hPa geopotential height

The 500-hPa geopotential height and anomalies, averaged over the duration of the Alaskan blocking events in the NCEP reanalysis, the CFS and AMIP simulations are shown in Fig. 1. Anomalies are calculated by removing the mean plus the first four harmonics of the respective 22 year

mean annual cycles. In general, the AMIP and CFS simulations compare favorably with observations. Both the AMIP and CFS simulations exhibit the negative 500-hPa height anomaly (i.e., enhanced storm track) equatorward of the blocking ridge, along with the downstream trough over North America and the ridging off the United States (US) east coast.

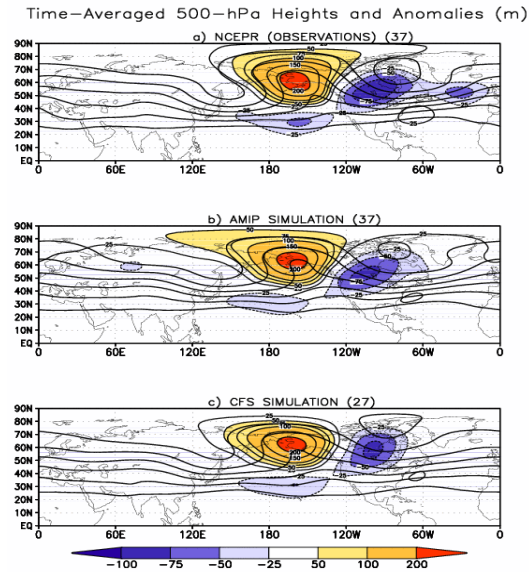


Fig. 1. Time-averaged 500-hPa geopotential height (contours) and anomalies (colored) averaged over the duration of all Alaskan blocking events in the (a) NCEP reanalysis, (b) AMIP simulation, and (c) CFS simulation. Units are meters, with solid (dashed) contours denoting positive (negative) anomalies.

One notable difference among the models is the more pronounced meridional flow, both upstream and downstream, in the NCEP reanalysis as compared to the AMIP and CFS simulations. In the CFS integration the flow pattern appears more zonal with less amplified downstream development.

b. Sea-Level Pressure

In Fig. 2 we compare the time-averaged sea-level pressure (SLP) anomalies among the 3 models. Again the anomalies are calculated by removing the first four harmonics of the respective 22-year mean annual cycles. A notable difference among the models is the pronounced eastward extension of the negative SLP anomaly toward the US west coast in the AMIP

simulation. Also, both the AMIP and CFS simulations have a smaller-scale and more northward positioned ridge off the US east coast. In the NCEP reanalysis the positive SLP anomalies associated with the blocking ridge appear to extend further southward into the southern Great Plains of North America. Implications for the precipitation distribution will be discussed below.

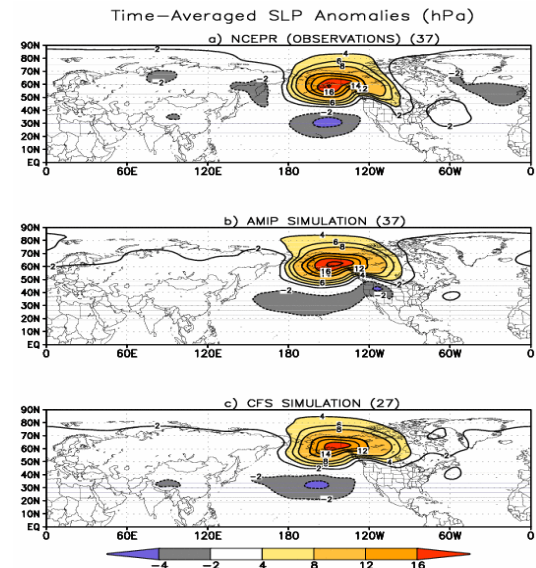


Fig. 2. Time-averaged sea-level pressure (SLP) anomalies in hPa, averaged over the duration of all Alaskan blocking events in the (a) NCEP reanalysis, (b) AMIP simulation and (c) CFS simulation. Positive (negative) contours are given in solid (dash).

c. Surface Temperature

A principal finding of the study by Carrera et al. (2004) was the significant shift in the daily mean surface temperature distribution during Alaskan blocking toward colder temperatures in the region extending from the Yukon southeastward to the southern plains of the US, associated with a reduced surface temperature variance. Similarly, over extreme western Alaska there was a shift in the daily mean surface temperature distribution toward warmer temperatures. The shift toward colder (warmer) daily mean surface temperatures during Alaskan blocking was also accompanied by a shift in the tails of the distribution toward more extreme cold (warm) days in these two regions.

Figure 3 compares the time-averaged surface temperature anomalies during the Alaskan blocking events among the 3 models.

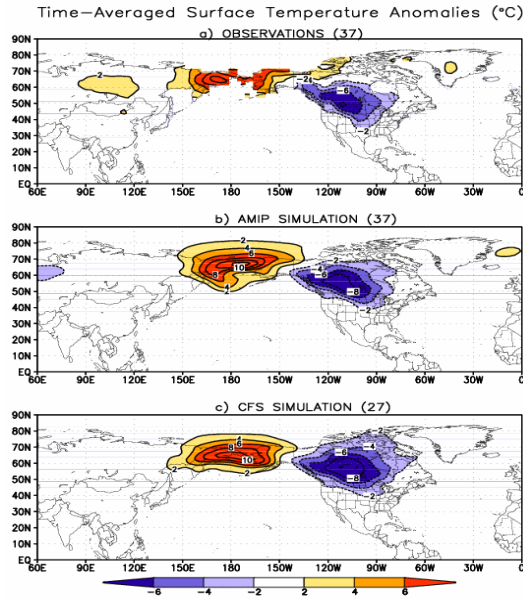


Fig. 3. Surface temperature anomalies ($^{\circ}\text{C}$), averaged over the duration of the Alaskan blocking events. (a) GTS surface temperature, (b) AMIP simulation and (c) CFS simulation. Positive (negative) contours denote positive (negative) anomalies.

Both the AMIP and CFS simulations compare favorably with observations, capturing the positive-negative surface temperature dipole pattern. The negative surface temperature anomalies appear to follow the orography over western North America, with the colder temperatures plunging further southward in the GTS dataset.

d. Precipitation and vertically integrated moisture transport

The presence of persistent positive height anomalies in the vicinity of Alaska has been linked to heavy precipitation over California and the southwestern US (Ely et al. 1994; Robertson and Ghil 1999). Carrera et al. (2004) found that the regions of Southern California, the Southwest and the Intermountain West all possessed a higher frequency of heavy precipitation days during Alaskan blocking when compared to the long-term winter climatology. In Fig. 4 we

present the time-averaged precipitation and vertically integrated moisture transport anomalies over the Alaskan blocking events from the regional reanalysis, and the AMIP and CFS simulations. Recall that the regional reanalysis assimilates observed precipitation and hence the precipitation structures should compare very well with observations. We were not able to calculate the vertically integrated moisture transport anomalies for the CFS simulation owing to the lack of a sufficient number of vertical levels.

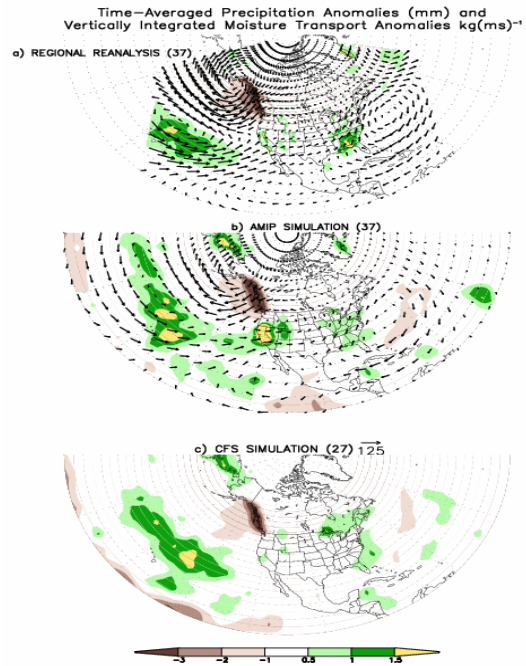


Fig. 4. Precipitation (shaded, mm day^{-1}) and vertically integrated moisture transport anomalies (kg (ms)^{-1}) averaged over the duration of the Alaskan blocking events. (a) regional reanalysis, (b) AMIP simulation, and (c) CFS simulation.

It is very encouraging to note that both the AMIP and CFS simulations are able to capture the enhanced precipitation associated with the equatorward displaced storm track. Both the AMIP and the CFS simulations also capture the strong negative precipitation anomalies along the British Columbia coastline. The CFS simulation fails to produce the enhanced precipitation over Southern California and the Southwest, while the AMIP simulation appears to precipitate too much, consistent with the eastward extended negative SLP anomaly

(Fig. 2b). Over the Ohio Valley and Southeast where Carrera et al. (2004) found a higher frequency of heavy precipitation events during the Alaskan blocking regime, both the AMIP and CFS simulate less precipitation than observed.

4.0 Future Work

The reason(s) why the CFS simulates a lower number of blocking events when compared with observed and the AMIP simulations needs further investigation. Carrera et al. (2004) found that the number of blocked days over the Alaskan region was sensitive to the phase of the ENSO cycle with a reduced (increased) number of blocked days during El Niño (La Niña/neutral) winters. Future work will examine the interannual variability of Alaskan blocking as it relates to the ENSO cycle in both the CFS and AMIP simulations.

5.0 References

- Carrera, M. L., R. W. Higgins, and V. E. Kousky, 2004: Downstream weather impacts associated with atmospheric blocking over the Northeast Pacific. *J. Climate*, in press.
- Chen, W. Y., and H. M. Van den Dool, 1995: Low-frequency anomalies in the NMC MRF model and reality. *J. Climate*, **8**, 1369-1385.
- D'Andrea, F. and Coauthors, 1998: Northern Hemisphere atmospheric blocking as simulated by 15 atmospheric general circulation models in the period 1979-1988. *Climate Dyn.*, **14**, 385-407.
- Dole, R. M., 1986: The life cycles of persistent anomalies and blocking over the North Pacific. *Advances in Geophysics*. Vol. 29, Academic Press, 31-69.
- Dole, R. M., and N. D. Gordon, 1983: Persistent anomalies of the extratropical Northern Hemisphere wintertime circulation: Geographical distribution and regional persistence characteristics. *Mon. Wea. Rev.*, **111**, 1567-1586.
- Ely, L. L., Y. Enzel, and D. R. Cayan, 1994: Anomalous North Pacific atmospheric circulation and large winter floods in the southwestern United States. *J. Climate*, **7**, 977-987.
- Higgins, R. W., and S. D. Schubert, 1994: Simulated life cycles of persistent anticyclonic anomalies over the North Pacific: Role of synoptic-scale eddies. *J. Atmos. Sci.*, **51**, 3238-3260.
- Higgins, R. W., and S. D. Schubert, 1996: Simulations of persistent North Pacific circulation anomalies and interhemispheric teleconnections. *J. Atmos. Sci.*, **53**, 188-207.
- Higgins, R. W., and K. C. Mo, 1997: Persistent circulation anomalies and the tropical intraseasonal oscillation. *J. Climate*, **10**, 223-244.
- Kalnay, E., and Coauthors, 1996: The NCEP/NCAR 40-Year Reanalysis Project. *Bull. Amer. Meteor. Soc.*, **77**, 437-471.
- Kistler, R. W., W. Collins, S. Saha, G. White, and J. Woollen, 2001: The NCEP-NCAR 50-Year Reanalysis: Monthly means CD-ROM and documentation. *Bull. Amer. Meteor. Soc.*, **82**, 247-268.
- Mesinger, F., and Coauthors, 2004: North American Regional Reanalysis. Paper P1.1 in 15th Symposium on Global Change and Climate Variations, American Meteorological Society, Seattle, WA, 11-15 January.
- Nakamura, H., and J. M. Wallace, 1990: Observed changes in baroclinic wave activity during the life cycles of low-frequency circulation anomalies. *J. Atmos. Sci.*, **47**, 1100-1116.
- Pelly, J. L., and B. J. Hoskins, 2003: How well does the ECMWF Ensemble Prediction System predict blocking? *Quart. J. Roy. Meteor. Soc.*, **129**, 1683-1702.
- Roberston, A. W., and M. Ghil, 1999: Large-scale weather regimes and local climate over the western United States. *J. Climate*, **12**, 1796-1813.
- Tibaldi, S. and F. Molteni, 1990: On the operational predictability of blocking. *Tellus*, **42A**, 343-365.
- Tibaldi, S., E. Tosi, A. Navarra, and L. Pedulli, 1994: Northern and Southern Hemisphere seasonal variability of blocking frequency and predictability. *Mon. Wea. Rev.*, **122**, 1971-2003.
- Watson, J. S., and S. J. Colucci, 2002: Evaluation of ensemble predictions of blocking in the NCEP Global Spectral Model. *Mon. Wea. Rev.*, **130**, 3008-3021.